

Power Allocation and Effective Capacity of AF Successive Relays

Mohammad Lari

Received: date / Accepted: date

Abstract In the relay based telecommunications with K relays between the source and destination, $K + 1$ time or frequency slots are required for a single frame transmission. However, without the relays, only one time or frequency slot is used for a single frame transmission. Therefore, despite the benefits of relaying systems, this type of communications is not efficient from the spectral efficiency viewpoint. One solution to reduce this issue might be the full-duplex (FD) relays. An old technique which is reconsidered recently to improve the spectral efficiency of telecommunication systems. However, FD relays have a certain complexity, so, some similar techniques such as successive relays with nearly the same performance but less complexity is taken into account now. In successive relaying systems, two relays between the source and destination are employed which receive the transmitted frames from the source and relay it to the destination successively. This structure generally acts like an FD relays. In this paper, the effective capacity performance of an amplify and forward (AF) successive relaying systems with power allocation strategy at the relays

Electrical and Computer Engineering Faculty
Semnan University, Semnan, Iran
Tel.: +9823-33383947
E-mail: m_lari@semnan.ac.ir

are studied perfectly. However, while the inter-rely interference (IRI) between two successive relays has to be managed well, the power allocation and the effective capacity is derived under different assumptions about the IRI. In this way, we assume weak or strong, short or long-term constraints on the IRI. Then we extract the optimal transmitted power at the relay to maximize the effective capacity under these constraints.

1 Introduction

Full-Duplex (FD) communications is a promising technique which offers to double the spectral efficiency of radio links [1]. This impressive capability can response part of the explosive demands for high data-rate services. Due to this and despite multiple drawbacks of FD implementation, this technique has been considered as a candidate for next generation 5G wireless networks [2]. In addition, FD can eliminate hidden terminal problem in ad-hoc networks, congestion, and large end-to-end delays [3]. Therefore, FD communication systems have attracted many attentions in research area recently [3]-[4].

Half-Duplex (HD) and FD are two ways for connecting terminals in a wireless network. Traditionally, HD terminals transmit or receive either at different times or over different frequency bands. Therefore, for a simple connection, two time or frequency slots are consumed. On the other hand and when the terminals support FD connection, transmission and reception can be accomplished simultaneously in a same time slot and frequency band. Therefore, resource consumption is reduced to the half of traditional HD links [3]-[4]. Clearly, in a dense environment with a large number of users, employment of FD terminals can release a high amount of resources and may lead to the significant increase in data rate of active users. However, self-interference (SI) from a transmitter to its own receiver is the evident result of using FD terminals. Hence, man-

agement and reduction of SI are vital for the practical implementation of FD systems [3]-[6]. Fortunately, recent researches show efficient techniques for SI reduction which were not possible until a few years ago [7]. So, new research like our present paper can be considered for the practical purpose completely.

Another challenging technology for next generation 5G wireless networks is relaying which can provide lower transmit powers, higher throughput, and extensive coverage [8]. However, relaying suffers from low spectral efficiency. For example, consider one-way transmission from a source to a destination together with K parallel relays. For complete transmission from the source and relays to the destination, $K + 1$ different time slots or frequency bands are required. This may be compared with direct transmission between the source and destination which uses only one time slot and frequency band. Here, FD devices (FD relays and FD destination) can be organized to reduce this weakness [9]. Therefore, FD relaying systems are of most interest among the other FD systems.

To alleviate the complexity of FD relays, some quasi FD schemes like successive relaying, two-way relaying or buffer aided relaying are investigated [3], [10]-[11]. These techniques try to mimic FD relaying via two HD relays. In successive relaying, two relays listen to the source and retransmit their received signal to the destination successively. In other words, in each time slot, one of the relays receives a new data frame from the source while the other relay forwards the previous data frame to the destination. Then, the role is swapped in the next time slot. In this way, a new data frame can be sent to the destination in each time slot as if FD relay was employed. In this situation, while transmission and reception of two relays occur in a same time slot and frequency band, the transmitted signal from one relay can disturb the received signal by the other relay simultaneously. Therefore, inter-relay interference (IRI) may

degrade the whole performance. So, it has to be managed well in successive relaying [12]-[13].

Due to high performance and simplicity of successive relaying, this paper concentrates on the power allocation of this scheme. Power allocation is widely take into account in different relay structures such as amplify and forward (AF) [14]-[15] or decode and forward (DF) [16]-[18] relaying and under various conditions such as HD [19]-[20] or FD [21]-[22] transmission mode. In all these papers, the transmitted power at the source and/or relays is optimized to achieve certain target under power constraints. Several optimization targets have been adopted, such as outage probability minimization, capacity maximization, and signal to noise ratio (SNR) maximization. More precisely, successive relaying is also attracted attention and has been investigated from different aspects [23]-[28]. For example in [23]-[25], the IRI suppression are studied and different schemes based on differential cancellation and network coding are proposed for two-path successive relays. In [26]-[27], the authors have examined the throughput rate of a successive relay network which is suffered by the IRI. Then in [28], a spectrum sharing scheme for overlaid wireless networks based on the DF successive relaying technique is proposed. However, power allocation and effective capacity in successive relaying in addition to IRI considerations is not investigated previously¹. Here, we study the power allocation of AF successive relays for effective capacity maximization. The effective capacity is more general than the ergodic capacity which is defined as a maximum constant arrival rate with the delay quality-of-service (QoS) guarantee [30]-[33]. Then, the allocated power is derived under short-term and long-term IRI constraints and compared with different allocation techniques with different QoS requirements. IRI is not always harmful, and, strong IRI is

¹ For a complete review of successive relaying, please refer to [29]

more desirable in some states [10]-[13]. Therefore, in the following, we assume both weak and strong IRI in our optimization problem separately.

This paper is organized as follows: First, the system model is introduced in Section 2, where, successive relaying and interference management in this scheme are discussed. In addition, channel model and the effective capacity are explained here. In Section 3, we plan our optimization problem to maximize the effective capacity under different power constraints and then, the optimal allocated power is obtained in this section. Finally, the simulation results are presented in Section 4, and Section 5 concludes the paper.

2 System Model

2.1 Successive Relaying

Successive relaying behavior is shown in Fig. 1, where two AF relay nodes R_1 and R_2 , cooperate the source node S, amplify its received signal and retransmit it to the destination D successively. The direct source to destination link is also ignored. For more details, we assume each data frame has T symbols $\{x_1, x_2, \dots, x_T\}$, which has to be transmitted from the source to the destination. The specific steps for each time slot are described as follows [12]:

- In the 1st time slot, S transmits x_1 , R_1 listens to x_1 from S and R_2 is silent (see Fig. 1(a)).
- In the 2nd time slot, S transmits x_2 , R_2 listens to x_2 from S while being interfered by x_1 from R_1 and R_1 amplifies and forwards x_1 to D (see Fig. 1(b)).
- In the 3rd time slot, S transmits x_3 , R_1 listens to x_3 from S while being interfered by x_2 from R_2 and R_2 amplifies and forwards x_2 to D (see Fig. 1(c)).

- In the t^{th} time slot (t is even), S transmits x_t , R_2 listens to x_t from S while being interfered by x_{t-1} from R_1 and R_1 amplifies and forwards x_{t-1} to D (see Fig. 1(d)).
- In the $t + 1^{\text{th}}$ time slot ($t + 1$ is odd), S transmits x_{t+1} , R_1 listens to x_{t+1} from S while being interfered by x_t from R_2 and R_2 amplifies and forwards x_t to D (see Fig. 1(e)).
- Finally, in the $T + 1^{\text{th}}$ time slot ($T + 1$ is odd), R_2 amplifies and forwards x_T to D (see Fig. 1(f)).

Now, we can observe that T symbols are transmitted from the source and received completely in $T + 1$ time slots by the destination. So, the multiplexing ratio becomes $T/(T + 1)$ which approaches 1 for a large number of symbols T . This leads to the high spectral efficiency as can be obtained in FD relaying systems. Except for the first and last time slots, relays provide interference for each other. Note that, for achieving high performance of relaying systems, this IRI has to be managed carefully.

2.2 Interference Management

For proper relaying system performance, management of IRI between two relays is essential. Hence, applying interference cancellation techniques such as interference alignment (IA) [34]-[35] or successive interference cancellation (SIC) [12] is strongly recommended. However for the sake of simplicity, we assume that the relays using SIC for IRI suppression and we explain the interference cancellation as follows: (a) When the IRI is weak, the relay does not attempt to remove the interference. So, the power of interference is added to the power of noise and the overall SNR is reduced slightly. (b) On the other hand, when the IRI is strong, the relay first detects the interferer signal. Then, subtracts the estimated interference from the received signal. Now, detection

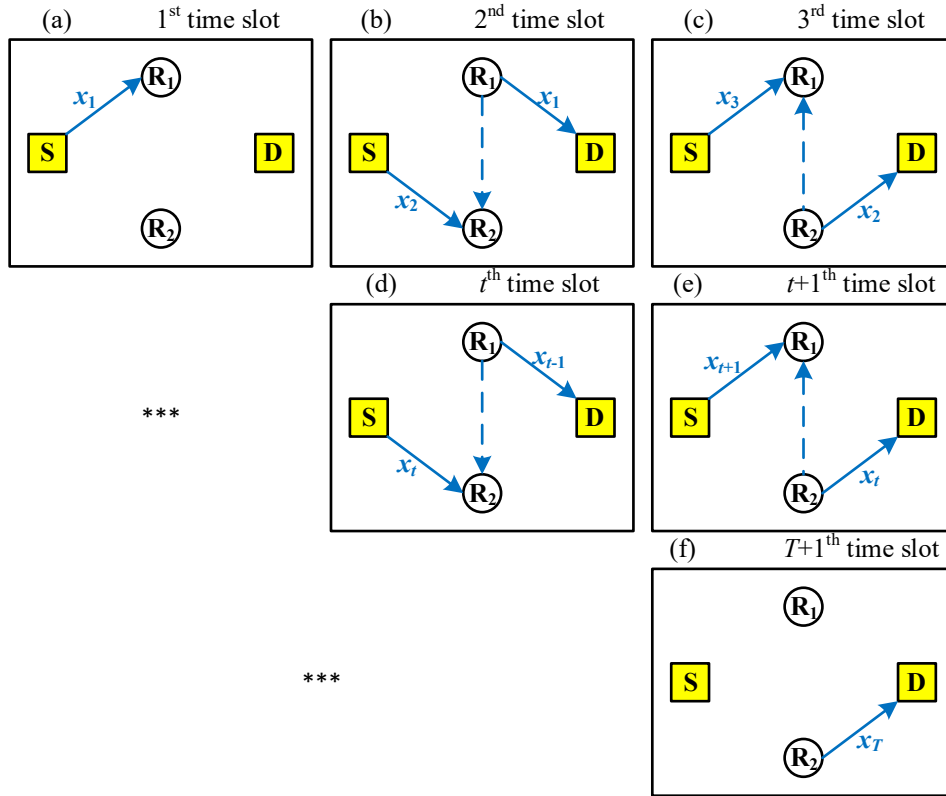


Fig. 1: Successive relaying in different time slots. Solid lines depicts the main paths and dashed lines show the interferer paths.

of the main signal without interference is possible. In this case, there will be no SNR reduction due to interference. Hence, the strong IRI is not damaging in this case.

Most of the time, interference is detrimental and interferer signal and symbols are discarded. However, this subject is not always the best solution. In our successive relaying scenario, the interference signal can be detected and used for further improvements. For example, according to description of 2.1, R₁ can extract just $\{x_1, x_3, \dots\}$ and R₂ can extract just $\{x_2, x_4, \dots\}$ when they transmitted from the source. Hence, these two relays do not have an access to

all symbols completely. But, by utilization of the IRI, R_1 and R_2 can obtain $\{x_2, x_4, \dots\}$ and $\{x_1, x_3, \dots\}$ respectively. Well, using the complete set of symbols in the relays, may lead to higher performance². Therefore, the strong IRI can be helpful in this scheme. For this reason, the strong IRI will be considered as one of the constraints in the optimization problem of section 3.

2.3 Channel Model

Here, we assume uncorrelated quasi-static flat fading channel, where, h_{SR_1} and h_{SR_2} denote $S - R_1$ and $S - R_2$ channel coefficients and h_{R_1D} and h_{R_2D} show $R_1 - D$ and $R_2 - D$ channel coefficients and $h_{R_1R_2}$ determines $R_1 - R_2$ channel coefficient respectively. The distances of $S - R_1$ and $S - R_2$ as well as $R_1 - D$ and $R_2 - D$ are nearly the same. Also, the average transmitted power by the source and each relay are assumed P_S and P_R and the power of additive white Gaussian noise (AWGN) is the same at the relays and destination. Therefore, the average SNR at the $S - R_1$ or $S - R_2$ link is $\bar{\gamma}_{SR}$ and at the $R_1 - D$ or $R_2 - D$ link is expressed as $\bar{\gamma}_{RD}$ and at the $R_1 - R_2$ link is written as $\bar{\gamma}_{IR}$. Now, assuming IRI cancellation with the SIC technique, the overall instantaneous SNR at the destination is written as [36]

$$\gamma_{eq} = \frac{\gamma_{SR}\gamma_{RD}}{\gamma_{SR} + \gamma_{RD} + 1} \quad (1)$$

where at the even time slots, $\gamma_{SR} = \bar{\gamma}_{SR}|h_{SR_1}|^2$ and $\gamma_{RD} = \bar{\gamma}_{RD}|h_{R_1D}|^2$ and at the odd time slots $\gamma_{SR} = \bar{\gamma}_{SR}|h_{SR_2}|^2$ and $\gamma_{RD} = \bar{\gamma}_{RD}|h_{R_2D}|^2$ respectively. In this way, the SNR at the link between the relays can be expressed as $\gamma_{IR} = \bar{\gamma}_{IR}|h_{R_1R_2}|^2$. In the Rayleigh fading channels, where $\bar{\gamma}_{SR} = \bar{\gamma}_{RD} = \bar{\gamma}$, the probability density function (PDF) and the cumulative distribution function

² The complete set of symbols can be used for channel estimation, higher order of diversity or ..., however, the details and method of using IRI is not our concern here in this paper.

(CDF) of the SNR are expressed as [36]

$$f_{\gamma_{\text{eq}}}(x) = e^{-2x/\bar{\gamma}} \frac{4x}{\bar{\gamma}^2} \left[K_1 \left(\frac{2x}{\bar{\gamma}} \right) + K_0 \left(\frac{2x}{\bar{\gamma}} \right) \right] \quad (2)$$

$$F_{\gamma_{\text{eq}}}(x) = 1 - e^{-2x/\bar{\gamma}} \frac{2x}{\bar{\gamma}} K_1 \left(\frac{2x}{\bar{\gamma}} \right) \quad (3)$$

where $K_1(\cdot)$ and $K_0(\cdot)$ are the first and zero-order modified Bessel function of the first kind respectively [37, eq. 8.407].

2.4 Effective Capacity

The effective capacity is a similar concept to the capacity which investigates the effect of transmitter and receiver buffer (queue) delay on the capacity [38]-[39]. In this regard, the effective capacity is defined as the maximum arrival rate that a wireless channel can support, in order to guarantee the QoS requirements such as the statistical delay constraint [38]-[39]. Consequently, the effective capacity is more realistic and can analyse the performance of the wireless channels against delay sensitive traffics more precisely.

For a dynamic queuing system with stationary and ergodic arrival and service processes, under sufficient conditions, the queue length process $Q(t)$ converges in distribution to a random variable $Q(\infty)$ such that [38]

$$\Pr\{Q(\infty) > q\} \approx \varepsilon e^{-\theta q} \quad (4)$$

for a large q , where ε represents the non-empty buffer probability, q determines a certain threshold and θ indicates the amount of required QoS. In addition, for the delay of a packet in the buffer as the main QoS metric, we have a similar probability function as [38]

$$\Pr\{D > d\} \approx \varepsilon e^{-\theta \delta d}, \quad (5)$$

where D indicates the tolerated delay, d is a delay-bound, and δ is jointly determined by both arrival and service processes. The statistical delay constraint in (5) represents the QoS which has to be guaranteed for the delay sensitive traffic sources. It is apparent that the QoS exponent θ has an important role here. Larger θ corresponds to more strict QoS constraint, while smaller θ implies looser QoS requirements.

Effective capacity provides the maximum constant arrival rate that can be supported by the time-varying wireless channel under the statistical delay constraint (5). Since the average arrival rate is equal to the average departure rate when the buffer is in a steady-state [38], the effective capacity can be viewed as the maximum throughput in the presence of such a constraint. With all these explanations, the effective capacity is defined as [38]-[39]

$$E_C(\theta) = -\frac{1}{\theta} \ln (\mathbf{E} \{e^{-\theta R}\}) \quad (6)$$

where R is the time-varying rate of the channel and $\mathbf{E}\{\cdot\}$ denotes the statistical expectation. For a specific application with a given statistical delay requirement, the QoS exponent θ can be determined from (5). Then, the maximum constant arrival rate of the sources that a wireless channel can support in order to guarantee the given QoS is concluded from (6). The power allocation scheme and the effective capacity of AF successive relaying are discussed in the next section.

3 Power Allocation Strategy

In order to maximize the effective capacity, the allocation power scheme at the relay is extracted here. As we explained before, high performance of successive relaying is obtained when the IRI is considered and managed well. So, we will assume weak or strong and short-term or long-term IRI constraints in

our optimization problem. Note that, weak constraint means the IRI is lower than the specific threshold q_0 and subsequently, strong constraint means the IRI is higher than the specific threshold q_0 . Besides, short-term constraint means the instantaneous IRI and long-term constraint means the average IRI respectively.

With power allocation strategy, we assume that the relays can adapt their transmitted power to maximize the effective capacity. In this regard, the relays transmit $\mu_0 P_R$ instead of P_R , where $\mu_0 \geq 0$ depicts the time-varying allocated power coefficient and we have $\mathbf{E}\{\mu_0\} = 1$ for constant average transmitted power. Now, with this policy, the instantaneous SNR at the destination is changed to

$$\tilde{\gamma}_{\text{eq}} = \frac{\gamma_{\text{SR}}\mu_0\gamma_{\text{RD}}}{\gamma_{\text{SR}} + \mu_0\gamma_{\text{RD}} + 1} \quad (7)$$

and the instantaneous capacity is written as

$$R = B \left(\frac{T}{T+1} \right) T_0 \log_2(1 + \tilde{\gamma}_{\text{eq}}) \quad (8)$$

where B specify the total required bandwidth and T_0 denotes one symbol duration or one transmission time slot in Fig. 1. Since T symbols are transmitted from the source to the destination in $T + 1$ time slots, the instantaneous capacity is written as (8). By substituting (8) into (6), the effective capacity of AF successive relays is obtained as

$$\begin{aligned} E_C(\theta) &= -\frac{1}{\theta} \ln \left(\mathbf{E} \left\{ e^{-\theta B \left(\frac{T}{T+1} \right) T_0 \log_2(1 + \tilde{\gamma}_{\text{eq}})} \right\} \right) \\ &= -\frac{1}{\theta} \ln \left(\mathbf{E} \left\{ e^{-\tilde{\theta} \ln(1 + \tilde{\gamma}_{\text{eq}})} \right\} \right) \\ &= -\frac{1}{\theta} \ln \left(\mathbf{E} \left\{ (1 + \tilde{\gamma}_{\text{eq}})^{-\tilde{\theta}} \right\} \right) \end{aligned} \quad (9)$$

where $\tilde{\theta} = \theta B \left(\frac{T}{T+1} \right) T_0 / \ln 2$. As we explained before, the IRI has a significant influence in the performance of successive relays and this interference has

to be managed properly. When the weak IRI is desirable, we can adjust the transmitted power of the relays to obtain the short-term or long-term interference below some specific threshold q_0 . Consequently, we use $\mu_0\gamma_{\text{IR}} \leq q_0$ as the short-term constraint or $\mathbb{E}\{\mu_0\gamma_{\text{IR}}\} \leq q_0$ for the long-term constraint as well. As the same way, when we need the strong IRI, we can adapt the transmitted power from the relays to obtain the short-term or long-term interference above the threshold q_0 . Therefore, we would have $\mu_0\gamma_{\text{IR}} \geq q_0$ as the short-term constraint or $\mathbb{E}\{\mu_0\gamma_{\text{IR}}\} \geq q_0$ for the long-term constraint, respectively. Now, we can summarize our optimization problem as

$$\begin{aligned} \mu_0^{\text{opt}} &= \arg \max_{\mu_0} -\frac{1}{\theta} \ln \left(\mathbb{E} \left\{ (1 + \tilde{\gamma}_{\text{eq}})^{-\tilde{\theta}} \right\} \right) \\ &= \arg \max_{\mu_0} -\frac{1}{\theta} \ln \left(\mathbb{E} \left\{ \left(1 + \frac{\gamma_{\text{SR}}\mu_0\gamma_{\text{RD}}}{\gamma_{\text{SR}} + \mu_0\gamma_{\text{RD}} + 1} \right)^{-\tilde{\theta}} \right\} \right) \end{aligned} \quad (10)$$

$$\text{s.t.} \quad \mu_0 \geq 0 \quad (11)$$

$$\mathbb{E}\{\mu_0\} = 1 \quad (12)$$

$$\mu_0\gamma_{\text{IR}} \leq q_0 \quad (13\text{a})$$

$$\mathbb{E}\{\mu_0\gamma_{\text{IR}}\} \leq q_0 \quad (13\text{b})$$

$$\mu_0\gamma_{\text{IR}} \geq q_0 \quad (13\text{c})$$

$$\mathbb{E}\{\mu_0\gamma_{\text{IR}}\} \geq q_0 \quad (13\text{d})$$

where (11) and (12) show the positive and constant average transmitted power constraints and (13) depicts the short-term and long-term IRI constraints respectively ((13a) shows the weak and short-term constraint, (13b) shows the weak and long-term constraint, (13c) shows the strong and short-term constraint and finally (13d) shows the strong and long-term constraint). Using

the Lagrangian optimization method [40], the problem can be solved and μ_0^{opt} is derived. However, applying the Lagrange method in the optimization problem of (10), a high non-linear equation of μ_0^{opt} is obtained and extraction of a closed-form solution for μ_0^{opt} is not possible [30]. Therefore, we continue with a novel approximation and replace μ_0 at the denominator of (10) by its average $\mathbb{E}\{\mu_0\} = 1$. Then, we can rewrite (10) as

$$\mu_0^{\text{opt}} = \arg \max_{\mu_0} -\frac{1}{\theta} \ln \left(\mathbb{E} \left\{ \left(1 + \frac{\gamma_{\text{SR}} \mu_0 \gamma_{\text{RD}}}{\gamma_{\text{SR}} + 1 \times \gamma_{\text{RD}} + 1} \right)^{-\bar{\theta}} \right\} \right) \quad (14)$$

and simplify it to

$$\mu_0^{\text{opt}} = \arg \max_{\mu_0} -\frac{1}{\theta} \ln \left(\mathbb{E} \left\{ (1 + \mu_0 \gamma_{\text{eq}})^{-\bar{\theta}} \right\} \right) \quad (15)$$

where γ_{eq} is introduced in (1). The constraints of the optimization remain unchanged. Now, we can obtain a closed-form solution for the allocated power in the following subsections.

3.1 Long-term IRI constraints

Now, we can use (11), (12) and (13b) for the weak and long-term IRI constraints. Here, the optimal power allocation is determined as

$$\mu_0^{\text{opt}} = \begin{cases} 0 & , \gamma_{\text{eq}} < \gamma_{\text{T}} \\ \left(\frac{1}{\gamma_{\text{T}}} \right)^{\frac{1}{\theta+1}} \left(\frac{1}{\gamma_{\text{eq}}} \right)^{\frac{\bar{\theta}}{\theta+1}} - \frac{1}{\gamma_{\text{eq}}} & , \gamma_{\text{eq}} \geq \gamma_{\text{T}} \end{cases} \quad (16)$$

where γ_{T} is a cut-off SNR threshold which is calculated from

$$\mathbb{E} \{ \mu_0^{\text{opt}} \} = \begin{cases} \frac{q_0}{\bar{\gamma}} & , q_0 < \bar{\gamma} \\ 1 & , q_0 \geq \bar{\gamma} \end{cases} . \quad (17)$$

Against, for the strong and long-term IRI constraints, we use (11), (12) and (13d) and obtain

$$\mu_0^{\text{opt}} = \begin{cases} 0 & , \gamma_{\text{eq}} < \gamma_{\text{T}} \\ \left(\frac{1}{\gamma_{\text{T}}}\right)^{\frac{1}{\theta+1}} \left(\frac{1}{\gamma_{\text{eq}}}\right)^{\frac{\bar{\theta}}{\theta+1}} - \frac{1}{\gamma_{\text{eq}}} & , \gamma_{\text{eq}} \geq \gamma_{\text{T}} \end{cases} \quad (18)$$

for the $q_0 \leq \bar{\gamma}$. Note that, when $q_0 > \bar{\gamma}$, the power allocation with all constraints (11), (12) and (13d) is impossible. The cut-off SNR threshold γ_{T} is calculated from $\text{E}\{\mu_0\} = 1$ (the proof of (16) has been derived in Appendix A and the proof of (18) is similar to Appendix A).

Finally, we can replace (16) or (18) into (15) to obtain the effective capacity of AF successive relays with the weak or strong long-term IRI constraints as follow (for the proof, please see Appendix B)

$$\begin{aligned} E_C(\theta) = & -\frac{1}{\theta} \ln \left\{ \frac{\sqrt{\pi}}{2\Gamma(5/2)} \left[F(3, 3/2, 5/2; 0) + \frac{1}{2} F(2, 1/2, 5/2; 0) \right] \right. \\ & - \frac{\sqrt{\pi}\gamma_{\text{T}}}{\bar{\gamma}} \left[G_{23}^{30} \left(\frac{4\gamma_{\text{T}}}{\bar{\gamma}} \middle| \begin{matrix} 0, 3/2 \\ -1, 2, 0 \end{matrix} \right) + G_{23}^{30} \left(\frac{4\gamma_{\text{T}}}{\bar{\gamma}} \middle| \begin{matrix} 0, 3/2 \\ -1, 1, 1 \end{matrix} \right) \right] \\ & + \frac{\sqrt{\pi}}{4} \left(\frac{4\gamma_{\text{T}}}{\bar{\gamma}} \right)^{\frac{1+2\bar{\theta}}{1+\theta}} \left[G_{23}^{30} \left(\frac{4\gamma_{\text{T}}}{\bar{\gamma}} \middle| \begin{matrix} 0, \frac{1}{2} + \frac{1}{1+\theta} \\ -1, 1 + \frac{1}{1+\theta}, -1 + \frac{1}{1+\theta} \end{matrix} \right) \right. \\ & \left. \left. + G_{23}^{30} \left(\frac{4\gamma_{\text{T}}}{\bar{\gamma}} \middle| \begin{matrix} 0, \frac{1}{2} + \frac{1}{1+\theta} \\ -1, \frac{1}{1+\theta}, \frac{1}{1+\theta} \end{matrix} \right) \right] \right\} \quad (19) \end{aligned}$$

where $F(., .; .; .)$ represents Gauss hypergeometric function [37, eq. 9.10], $\Gamma(\cdot)$ denotes the Gamma function and $G_{p,q}^{m,n}(\cdot)$ is the Meijer's G function defined in [37, eq. 9.301] which is easily evaluated using the popular numerical softwares.

3.2 Short-term IRI constraints

When the weak and short-term IRI is required, the constraints of (11), (12) and (13a) can be used and the optimal allocated power is obtained as

$$\mu_0^{\text{opt}} = \begin{cases} 0 & , \gamma_{\text{eq}} < \gamma_{\text{T}} \\ \left(\frac{1}{\gamma_{\text{T}}}\right)^{\frac{1}{\theta+1}} \left(\frac{1}{\gamma_{\text{eq}}}\right)^{\frac{\bar{\theta}}{\theta+1}} - \frac{1}{\gamma_{\text{eq}}} & , \gamma_{\text{eq}} \geq \gamma_{\text{T}}, \gamma_{\text{IR}} < \gamma_{\text{IR}}^* \\ \frac{q_0}{\gamma_{\text{IR}}} & , \gamma_{\text{eq}} \geq \gamma_{\text{T}}, \gamma_{\text{IR}} \geq \gamma_{\text{IR}}^* \end{cases} \quad (20)$$

On the other hand, with the strong and short-term IRI assumption, the constraints of (11), (12) and (13c) can be used to calculate the optimal allocated power as

$$\mu_0^{\text{opt}} = \begin{cases} 0 & , \gamma_{\text{eq}} < \gamma_{\text{T}} \\ \frac{q_0}{\gamma_{\text{IR}}} & , \gamma_{\text{eq}} \geq \gamma_{\text{T}}, \gamma_{\text{IR}} < \gamma_{\text{IR}}^* \\ \left(\frac{1}{\gamma_{\text{T}}}\right)^{\frac{1}{\theta+1}} \left(\frac{1}{\gamma_{\text{eq}}}\right)^{\frac{\bar{\theta}}{\theta+1}} - \frac{1}{\gamma_{\text{eq}}} & , \gamma_{\text{eq}} \geq \gamma_{\text{T}}, \gamma_{\text{IR}} \geq \gamma_{\text{IR}}^* \end{cases} \quad (21)$$

Here, γ_{T} is a cut-off SNR threshold which is determined from the average transmitted power, $E\{\mu_0\} = 1$, and γ_{IR}^* is ³

$$\gamma_{\text{IR}}^* = \frac{q_0}{\left(\frac{1}{\gamma_{\text{T}}}\right)^{\frac{1}{\theta+1}} \left(\frac{1}{\gamma_{\text{eq}}}\right)^{\frac{\bar{\theta}}{\theta+1}} - \frac{1}{\gamma_{\text{eq}}}}. \quad (22)$$

Finally, (20) or (21) can be replaced into (15) and the effective capacity of AF successive relays with the weak or strong short-term IRI constraints is obtained. Here, finding a closed-form solution for the effective capacity is not straightforward.

³ The proof of (21) and (22) is very similar to Appendix A.

4 Simulation Results

For the simulation we assume $B = 100\text{KHz}$, $T_0 = 1\text{msec}$ and $\frac{T}{T+1} \approx 1$ and for more simple drawing, the normalized effective capacity $\overline{E_C(\theta)} = E_C(\theta)/(BT_0)$ is plotted in the following figures.

The effective capacity of AF successive relays with the weak and long-term IRI constraints (see eq. (13b)) is plotted in Fig. 2 when $\bar{\gamma} = 10\text{dB}$ with $q_0 = 5\text{dB}$, $q_0 = 8\text{dB}$ and $q_0 \geq 10\text{dB}$ and also in Fig. 3 when we have $\bar{\gamma} = 20\text{dB}$ and $q_0 = 5\text{dB}$, $q_0 = 15\text{dB}$ and $q_0 \geq 20\text{dB}$ respectively. We can see the tight agreement between theory and simulation results in these figures which verifies the derived closed-form solution of the effective capacity in section 3.1. In addition, as we expected, the effective capacity increases when the threshold q_0 increases. Note that, when q_0 increases, the amount of tolerable interference between relays increases as well and therefore, the effective capacity of AF successive relay is increased.

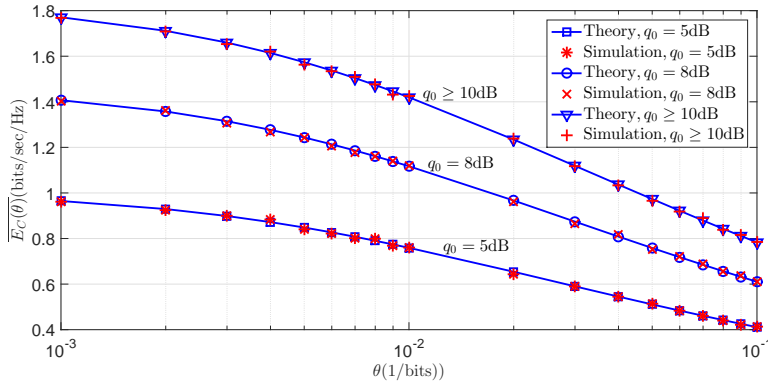


Fig. 2: Effective capacity in successive AF relays with the weak and long-term IRI constraints. We assume $\bar{\gamma} = 10\text{dB}$ with $q_0 = 5\text{dB}$, $q_0 = 8\text{dB}$ and $q_0 \geq 10\text{dB}$ here.

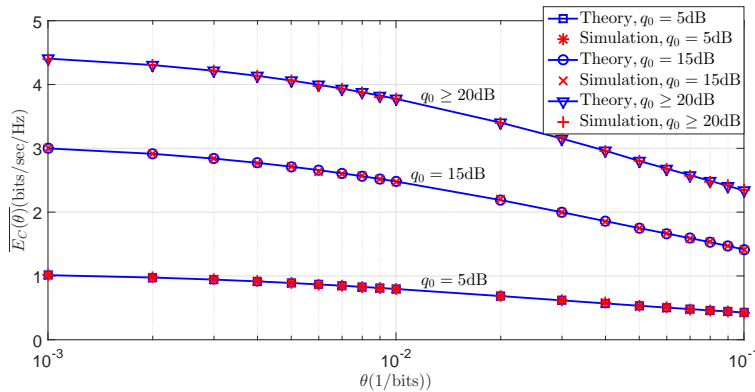


Fig. 3: Effective capacity in successive AF relays with the weak and long-term IRI constraints. We assume $\bar{\gamma} = 20\text{dB}$ with $q_0 = 5\text{dB}$, $q_0 = 15\text{dB}$ and $q_0 \geq 20\text{dB}$ here.

In a similar way, the effective capacity of AF successive relays with the strong and long-term IRI constraints (see eq. (13d)) is plotted in Fig. 4. Note that, the power allocation is not possible when $q_0 > \bar{\gamma}$, because the strong constrain is not realized in this situation. Full agreement between theory and simulation is also clear in Fig. 4.

After that, the effective capacity with the weak but short-term IRI constraints (see eq. (13a)) is plotted in Fig. 5 for $\bar{\gamma} = 10\text{dB}$ and Fig. 6 for $\bar{\gamma} = 20\text{dB}$ for different values of q_0 . We can observe that the effective capacity increases when the amount of acceptable IRI is increased. Without strict constraint on the interference, the relay can transmit more power temporally to improve the total effective capacity or requested QoS.

Now, we can compare the obtained results in Fig. 2 and 3 with the results of Fig. 5 and 6 accurately. Generally, the effective capacity with the long-term constraint outperforms the results with the short-term constraint. However, despite the obtained results, short-term constraint is necessary in some sensitive applications and can not be ignored ever. In addition, when θ increases

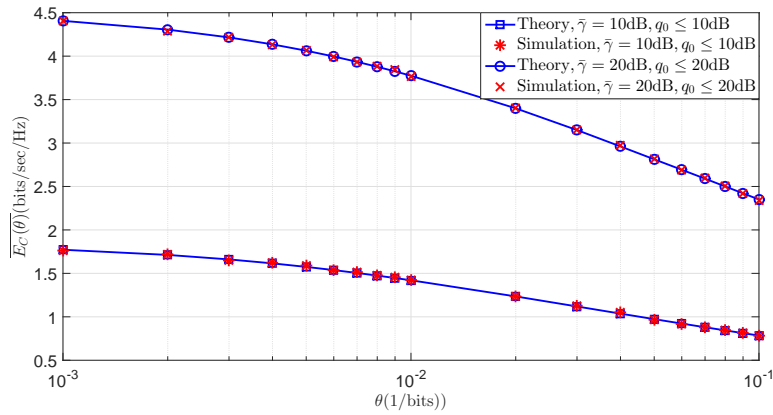


Fig. 4: Effective capacity in successive AF relays with the strong and long-term IRI constraints. We assume $\bar{\gamma} = 10\text{dB}$ with $q_0 \leq 10\text{dB}$ and $\bar{\gamma} = 20\text{dB}$ with $q_0 \leq 20\text{dB}$ here.

and high QoS is required, the effective capacity of successive AF relay with short-term IRI constraint drops rapidly. Therefore, we can conclude that the performance with the high QoS and short-term constraint is not suitable at all, and long-term constraint for management of interference is recommended for this situation properly.

In a similar way, the effective capacity with the strong and short-term IRI constraints (see eq. (13c)), can be drawn and compared with Fig. 4. However to avoid duplication, this figure is not plotted here.

For more details, in Fig. 7, we have drawn the effective capacity of AF successive relays with the optimal power allocation (16), constant power allocation $\mu_0 = 1$ and truncated channel inversion with

$$\mu_0 = \begin{cases} 0 & , \gamma_{\text{IR}} < \gamma_{\text{T}} \\ \frac{q_0}{\gamma_{\text{IR}}} & , \gamma_{\text{IR}} \geq \gamma_{\text{T}} \end{cases} \quad (23)$$

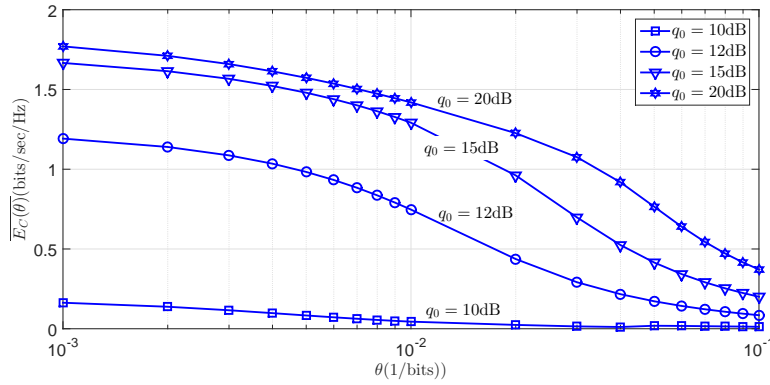


Fig. 5: Effective capacity in successive AF relays with the weak and short-term IRI constraints with $\bar{\gamma} = 10\text{dB}$ and $q_0 = 10\text{dB}$, $q_0 = 12\text{dB}$, $q_0 = 15\text{dB}$ and $q_0 = 20\text{dB}$.

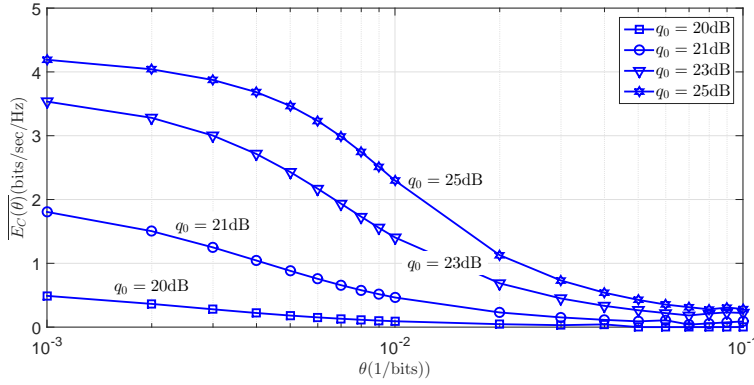


Fig. 6: Effective capacity in successive AF relays with the weak and short-term IRI constraints with $\bar{\gamma} = 20\text{dB}$ and $q_0 = 20\text{dB}$, $q_0 = 21\text{dB}$, $q_0 = 23\text{dB}$ and $q_0 = 25\text{dB}$.

where γ_T is obtained from $E\{\mu_0\} = 1$. In constant power allocation technique, there is no constraint on the IRI. So, the performance at low value of θ with loose QoS, tends to the performance with the optimal power allocation. However, at high value of θ , the performance with the optimal power allocation, outperforms the other techniques of transmission. In addition, when truncated

channel inversion technique is used, the IRI can remain constant but the effective capacity performance is very poor. Therefore, the optimal power allocation (similar to (16)) at the relay is strongly recommended specially when high QoS is required.

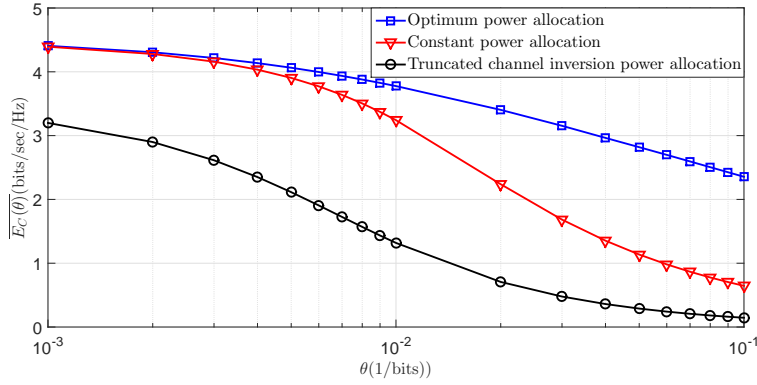


Fig. 7: Comparison of the effective capacity with different power allocation techniques when $\bar{\gamma} = 20\text{dB}$ and $q_0 = 20\text{dB}$.

Finally, the effective capacity of successive AF relaying scheme is compared with the traditional HD relaying in Fig. 8 versus QoS exponent θ . For the successive relays we assume the weak and long-term constraint and optimal power allocation (16) with $q_0 = 5\text{dB}$ or $q_0 = 15\text{dB}$ or $q_0 = 20\text{dB}$. On the other hand, in the HD mode, there is no IRI and therefore, the optimal power allocation coefficient μ_0 can be obtained from (16) when q_0 tends to very small value (i.e. $q_0 \rightarrow -\infty$). As we expected, we can see that successive relaying outperforms the traditional HD relaying especially when we manage the IRI with high value of threshold q_0 (i.e. $q_0 = 20\text{dB}$). When the threshold q_0 decreases and more strict constraint on the IRI is required, the effective capacity of successive relays decreases and approaches the effective capacity of HD relaying.

However at low value of q_0 when the IRI is not tolerable, using HD relaying is more efficient than the successive relays.

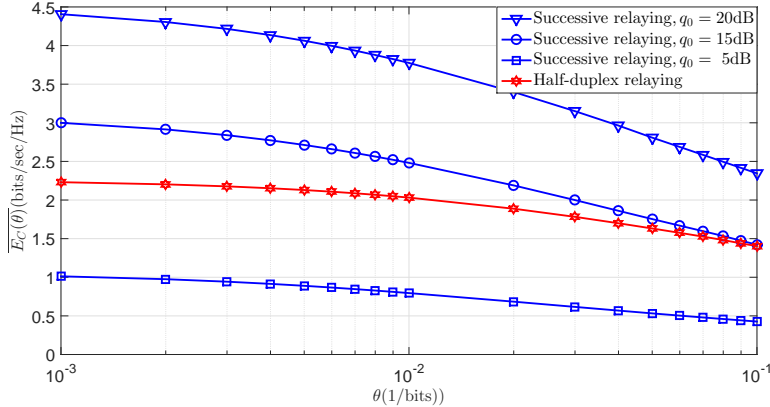


Fig. 8: Comparison of the effective capacity with the successive AF relays and HD relays when $\bar{\gamma} = 20$ dB.

5 Conclusion

In this paper, power allocation at the successive relay is studied. Successive relaying can be considered as a simple form of full-duplex relay implementation. In the successive relaying technique, two half-duplex relays with successive retransmission, act like a full-duplex relay. However, inter-relay interference management is crucial for proper operation of this technique. Here, the power allocation in AF successive relays for the effective capacity maximization was the goal. So, first, the power allocation coefficient with the long-term inter-relay interference constraint is calculated and a closed-form solution for the effective capacity is derived. Then, the power allocation with the short-term constraint is extracted. Finally, the effective capacity with the different type of power allocation is compared and we observed that in high QoS and low

latency requirement, interference management with long-term constraint have a better performance and effective capacity results.

A Proof of (16)

First, we can write the optimization problem in a standard form as

$$\begin{aligned} & \max_{\mu_0} -\mathbf{E} \left\{ (1 + \mu_0 \gamma_{\text{eq}})^{-\tilde{\theta}} \right\} \\ \text{s.t.} \quad & \mathbf{E} \{ \mu_0 \} \leq 1, \quad \mathbf{E} \{ \mu_0 \gamma_{\text{IR}} \} \leq q_0 \\ & -\mu_0 \leq 0. \end{aligned} \quad (24)$$

Then, using Lagrangian method, the cost function is written as

$$J = -\mathbf{E} \left\{ (1 + \mu_0 \gamma_{\text{eq}})^{-\tilde{\theta}} \right\} + \lambda_1 (1 - \mathbf{E} \{ \mu_0 \}) + \lambda_2 (q_0 - \mathbf{E} \{ \mu_0 \gamma_{\text{IR}} \}) + \lambda_3 \mu_0 \quad (25)$$

where $\lambda_1 \geq 0$, $\lambda_2 \geq 0$ and $\lambda_3 \geq 0$ are the nonnegative Lagrange multipliers corresponding to our constraints. Taking the partials with respect to μ_0 , we will have [40]

$$\begin{aligned} \frac{\partial J}{\partial \mu} &= \mathbf{E} \left\{ \tilde{\theta} \gamma_{\text{eq}} (1 + \mu_0 \gamma_{\text{eq}})^{-\tilde{\theta}-1} \right\} - \lambda_1 - \lambda_2 \mathbf{E} \{ \gamma_{\text{IR}} \} + \lambda_3 \\ &= \mathbf{E} \left\{ \tilde{\theta} \gamma_{\text{eq}} (1 + \mu_0 \gamma_{\text{eq}})^{-\tilde{\theta}-1} \right\} - \lambda_1 - \lambda_2 \bar{\gamma} + \lambda_3. \end{aligned} \quad (26)$$

Now, we can find μ_0^{opt} , λ_1^{opt} , λ_2^{opt} and λ_3^{opt} such that

$$\mathbf{E} \left\{ \tilde{\theta} \gamma_{\text{eq}} (1 + \mu_0^{\text{opt}} \gamma_{\text{eq}})^{-\tilde{\theta}-1} \right\} - \lambda_1^{\text{opt}} - \lambda_2^{\text{opt}} \bar{\gamma} + \lambda_3^{\text{opt}} = 0 \quad (27)$$

and

$$\lambda_1^{\text{opt}} (1 - \mathbf{E} \{ \mu_0^{\text{opt}} \}) = 0 \quad (28)$$

$$\lambda_2^{\text{opt}} (q_0 - \mathbf{E} \{ \mu_0^{\text{opt}} \gamma_{\text{IR}} \}) = 0 \quad (29)$$

and

$$\lambda_3^{\text{opt}} \mu_0^{\text{opt}} = 0 \quad (30)$$

correspondingly. From (30), since $\mu_0^{\text{opt}} = 0$ is not acceptable, we can conclude that $\lambda_3^{\text{opt}} = 0$.

Consider (28) and (29), we can break the analysis into four different cases as follows.

1. If $\lambda_1^{\text{opt}} = 0$ ($1 - \mathbb{E}\{\mu_0^{\text{opt}}\} \neq 0$) and $\lambda_2^{\text{opt}} = 0$ ($q_0 - \mathbb{E}\{\mu_0^{\text{opt}}\gamma_{\text{IR}}\} \neq 0$), then (27) converts to $\mathbb{E}\left\{\tilde{\theta}\gamma_{\text{eq}}\left(1 + \mu_0^{\text{opt}}\gamma_{\text{eq}}\right)^{-\tilde{\theta}-1}\right\} = 0$. Since we assume $\tilde{\theta} > 0$, $\mu_0^{\text{opt}} > 0$, $\gamma_{\text{eq}} > 0$ and $\gamma_{\text{IR}} > 0$, this case is not a feasible solution.
2. If $\lambda_1^{\text{opt}} = 0$ ($1 - \mathbb{E}\{\mu_0^{\text{opt}}\} \neq 0$) and $q_0 - \mathbb{E}\{\mu_0^{\text{opt}}\gamma_{\text{IR}}\} = 0$ ($\lambda_2^{\text{opt}} \neq 0$), then (27) converts to $\mathbb{E}\left\{\tilde{\theta}\gamma_{\text{eq}}\left(1 + \mu_0^{\text{opt}}\gamma_{\text{eq}}\right)^{-\tilde{\theta}-1}\right\} = \lambda_2^{\text{opt}}\bar{\gamma}$. Here, we can assume $\tilde{\theta}\gamma_{\text{eq}}\left(1 + \mu_0^{\text{opt}}\gamma_{\text{eq}}\right)^{-\tilde{\theta}-1} = \lambda_2^{\text{opt}}\bar{\gamma}$ and $\mu_0^{\text{opt}} > 0$ which leads to

$$\mu_0^{\text{opt}} = \begin{cases} 0 & , \gamma_{\text{eq}} < \frac{\lambda_2^{\text{opt}}\bar{\gamma}}{\tilde{\theta}} \\ \left(\frac{\tilde{\theta}}{\lambda_2^{\text{opt}}\bar{\gamma}}\right)^{\frac{1}{\tilde{\theta}+1}} \left(\frac{1}{\gamma_{\text{eq}}}\right)^{\frac{\tilde{\theta}}{\tilde{\theta}+1}} - \frac{1}{\gamma_{\text{eq}}} & , \gamma_{\text{eq}} \geq \frac{\lambda_2^{\text{opt}}\bar{\gamma}}{\tilde{\theta}} \end{cases}. \quad (31)$$

Note that, λ_2^{opt} can be calculated from $\mathbb{E}\{\mu_0^{\text{opt}}\gamma_{\text{IR}}\} = \mathbb{E}\{\mu_0^{\text{opt}}\}\bar{\gamma} = q_0$ or equivalently $\mathbb{E}\{\mu_0^{\text{opt}}\} = q_0/\bar{\gamma}$. Since we assumed $\lambda_1^{\text{opt}} = 0$, then we have $\mathbb{E}\{\mu_0^{\text{opt}}\} < 1$. Therefore, this case is valid when $q_0/\bar{\gamma} < 1$.

3. If $\lambda_2^{\text{opt}} = 0$ ($q_0 - \mathbb{E}\{\mu_0^{\text{opt}}\gamma_{\text{IR}}\} \neq 0$) and $1 - \mathbb{E}\{\mu_0^{\text{opt}}\} = 0$ ($\lambda_1^{\text{opt}} \neq 0$), then (27) converts to $\mathbb{E}\left\{\tilde{\theta}\gamma_{\text{eq}}\left(1 + \mu_0^{\text{opt}}\gamma_{\text{eq}}\right)^{-\tilde{\theta}-1}\right\} = \lambda_1^{\text{opt}}$. Here, we can assume $\tilde{\theta}\gamma_{\text{eq}}\left(1 + \mu_0^{\text{opt}}\gamma_{\text{eq}}\right)^{-\tilde{\theta}-1} = \lambda_1^{\text{opt}}$ and $\mu_0^{\text{opt}} > 0$ which leads to

$$\mu_0^{\text{opt}} = \begin{cases} 0 & , \gamma_{\text{eq}} < \frac{\lambda_1^{\text{opt}}}{\tilde{\theta}} \\ \left(\frac{\tilde{\theta}}{\lambda_1^{\text{opt}}}\right)^{\frac{1}{\tilde{\theta}+1}} \left(\frac{1}{\gamma_{\text{eq}}}\right)^{\frac{\tilde{\theta}}{\tilde{\theta}+1}} - \frac{1}{\gamma_{\text{eq}}} & , \gamma_{\text{eq}} \geq \frac{\lambda_1^{\text{opt}}}{\tilde{\theta}} \end{cases}. \quad (32)$$

Note that, λ_1^{opt} can be calculated from $\mathbb{E}\{\mu_0^{\text{opt}}\} = 1$. Since we assumed $\lambda_2^{\text{opt}} = 0$, then we have $\mathbb{E}\{\mu_0^{\text{opt}}\gamma_{\text{IR}}\} = \mathbb{E}\{\mu_0^{\text{opt}}\}\bar{\gamma} < q_0$. Therefore, this case is valid when $q_0/\bar{\gamma} > 1$.

4. If $1 - \mathbb{E}\{\mu_0^{\text{opt}}\} = 0$ ($\lambda_1^{\text{opt}} \neq 0$) and $q_0 - \mathbb{E}\{\mu_0^{\text{opt}}\gamma_{\text{IR}}\} = 0$ ($\lambda_2^{\text{opt}} \neq 0$), then (27) converts to $\mathbb{E}\left\{\tilde{\theta}\gamma_{\text{eq}}\left(1 + \mu_0^{\text{opt}}\gamma_{\text{eq}}\right)^{-\tilde{\theta}-1}\right\} = \lambda_1^{\text{opt}} + \lambda_2^{\text{opt}}\bar{\gamma}$. Here, we can assume $\tilde{\theta}\gamma_{\text{eq}}\left(1 + \mu_0^{\text{opt}}\gamma_{\text{eq}}\right)^{-\tilde{\theta}-1} = \lambda_1^{\text{opt}} + \lambda_2^{\text{opt}}\bar{\gamma} = \ell$ and $\mu_0^{\text{opt}} > 0$ which leads to

$$\mu_0^{\text{opt}} = \begin{cases} 0 & , \gamma_{\text{eq}} < \frac{\ell}{\tilde{\theta}} \\ \left(\frac{\tilde{\theta}}{\ell}\right)^{\frac{1}{\tilde{\theta}+1}} \left(\frac{1}{\gamma_{\text{eq}}}\right)^{\frac{\tilde{\theta}}{\tilde{\theta}+1}} - \frac{1}{\gamma_{\text{eq}}} & , \gamma_{\text{eq}} \geq \frac{\ell}{\tilde{\theta}} \end{cases}. \quad (33)$$

Note that, ℓ can be calculated from both $\mathbb{E}\{\mu_0^{\text{opt}}\} = 1$ or $\mathbb{E}\{\mu_0^{\text{opt}}\gamma_{\text{IR}}\} = \mathbb{E}\{\mu_0^{\text{opt}}\}\bar{\gamma} = q_0$ with the same value. Therefore, this case is valid when $q_0/\bar{\gamma} = 1$.

Now, we can aggregate cases 2, 3 and 4 in one case such as

$$\mu_0^{\text{opt}} = \begin{cases} 0 & , \gamma_{\text{eq}} < \gamma_{\text{T}} \\ \left(\frac{1}{\gamma_{\text{T}}}\right)^{\frac{1}{\theta+1}} \left(\frac{1}{\gamma_{\text{eq}}}\right)^{\frac{\tilde{\theta}}{\theta+1}} - \frac{1}{\gamma_{\text{eq}}} & , \gamma_{\text{eq}} \geq \gamma_{\text{T}} \end{cases} \quad (34)$$

where γ_{T} is a cut-off SNR threshold which is determined from

$$\mathbb{E} \left\{ \mu_0^{\text{opt}} \right\} = \begin{cases} \frac{q_0}{\bar{\gamma}} & , q_0 < \bar{\gamma} \\ 1 & , q_0 \geq \bar{\gamma} \end{cases} \quad (35)$$

B Proof of (19)

By substituting (16) or (18) into (15), we will have

$$\mathbb{E} \left\{ \left(1 + \mu_0^{\text{opt}} \gamma_{\text{eq}} \right)^{-\tilde{\theta}} \right\} = \underbrace{\int_0^{\gamma_{\text{T}}} f_{\gamma_{\text{eq}}}(x) dx}_{I_1} + \underbrace{\int_{\gamma_{\text{T}}}^{\infty} (x/\gamma_{\text{T}})^{-\tilde{\theta}/(1+\tilde{\theta})} f_{\gamma_{\text{eq}}}(x) dx}_{I_2} \quad (36)$$

where $f_{\gamma_{\text{eq}}}(x)$ is presented in (2). For solving I_1 , it can be changed to two infinite integrals as

$$\begin{aligned} I_1 &= \underbrace{\int_0^{\infty} f_{\gamma_{\text{eq}}}(x) dx}_{I_3} - \underbrace{\int_{\gamma_{\text{T}}}^{\infty} f_{\gamma_{\text{eq}}}(x) dx}_{I_4} \\ &= \frac{\sqrt{\pi}}{2\Gamma(5/2)} \left[F(3, 3/2, 5/2; 0) + \frac{1}{2} F(2, 1/2, 5/2; 0) \right] \\ &\quad - \frac{\sqrt{\pi} \gamma_{\text{T}}}{\bar{\gamma}} \left[G_{23}^{30} \left(\frac{4\gamma_{\text{T}}}{\bar{\gamma}} \left| \begin{matrix} 0, 3/2 \\ -1, 2, 0 \end{matrix} \right. \right) + G_{23}^{30} \left(\frac{4\gamma_{\text{T}}}{\bar{\gamma}} \left| \begin{matrix} 0, 3/2 \\ -1, 1, 1 \end{matrix} \right. \right) \right] \end{aligned} \quad (37)$$

where the closed-form solution of I_3 and I_4 is possible using [37, eq. 6.621-3] and [37, eq. 6.625-7], respectively. Once again [37, eq. 6.625-7] can be used for finding I_2 . Therefore, we have

$$\begin{aligned} I_2 &= \frac{\sqrt{\pi}}{4} \left(\frac{4\gamma_{\text{T}}}{\bar{\gamma}} \right)^{\frac{1+2\tilde{\theta}}{1+\tilde{\theta}}} \left[G_{23}^{30} \left(\frac{4\gamma_{\text{T}}}{\bar{\gamma}} \left| \begin{matrix} 0, \frac{1}{2} + \frac{1}{1+\tilde{\theta}} \\ -1, 1 + \frac{1}{1+\tilde{\theta}}, -1 + \frac{1}{1+\tilde{\theta}} \end{matrix} \right. \right) \right. \\ &\quad \left. + G_{23}^{30} \left(\frac{4\gamma_{\text{T}}}{\bar{\gamma}} \left| \begin{matrix} 0, \frac{1}{2} + \frac{1}{1+\tilde{\theta}} \\ -1, \frac{1}{1+\tilde{\theta}}, \frac{1}{1+\tilde{\theta}} \end{matrix} \right. \right) \right] \end{aligned} \quad (38)$$

where $F(\cdot, \cdot; \cdot; \cdot)$ represents Gauss hypergeometric function [37, eq. 9.10], $\Gamma(\cdot)$ denotes the Gamma function and $G_{p,q}^{m,n}(\cdot)$ is the Meijer's G function defined in [37, eq. 9.301]. Now, connecting the obtained results for I_1 and I_2 , we have

$$\begin{aligned}
E_C(\theta) = & -\frac{1}{\theta} \ln \left\{ \frac{\sqrt{\pi}}{2\Gamma(5/2)} \left[F(3, 3/2, 5/2; 0) + \frac{1}{2} F(2, 1/2, 5/2; 0) \right] \right. \\
& - \frac{\sqrt{\pi}\gamma_T}{\bar{\gamma}} \left[G_{23}^{30} \left(\frac{4\gamma_T}{\bar{\gamma}} \left| \begin{matrix} 0, 3/2 \\ -1, 2, 0 \end{matrix} \right. \right) + G_{23}^{30} \left(\frac{4\gamma_T}{\bar{\gamma}} \left| \begin{matrix} 0, 3/2 \\ -1, 1, 1 \end{matrix} \right. \right) \right] \\
& + \frac{\sqrt{\pi}}{4} \left(\frac{4\gamma_T}{\bar{\gamma}} \right)^{\frac{1+2\bar{\theta}}{1+\theta}} \left[G_{23}^{30} \left(\frac{4\gamma_T}{\bar{\gamma}} \left| \begin{matrix} 0, \frac{1}{2} + \frac{1}{1+\theta} \\ -1, 1 + \frac{1}{1+\theta}, -1 + \frac{1}{1+\theta} \end{matrix} \right. \right) \right. \\
& \left. \left. + G_{23}^{30} \left(\frac{4\gamma_T}{\bar{\gamma}} \left| \begin{matrix} 0, \frac{1}{2} + \frac{1}{1+\theta} \\ -1, \frac{1}{1+\theta}, \frac{1}{1+\theta} \end{matrix} \right. \right) \right] \right\}. \tag{39}
\end{aligned}$$

References

1. M. Pashazadeh and F. S. Tabataba, "Impact of loop-back interference and channel estimation errors on full-duplex relay networks," *Springer Wireless Netw.*, DoI: 10.1007/s11276-016-1205-3, Feb. 2016.
2. Z. Zhang, X. Chai, K. Long, A. V. Vasilakos and L. Hanzo, "Full duplex techniques for 5G networks: self-interference cancellation, protocol design, and relay selection," *IEEE Commun. Mag.*, vol. 53, no. 5, pp. 2-10, May 2015.
3. G. Liu, F. R. Yu, H. Ji and V. C. M. Leung, "In-band full-duplex relaying: A survey, research issues and challenges," *IEEE Commun. Surveys Tuts.*, vol. 17, no. 2, pp. 500-524, 2nd quarter 2015.
4. A. Sabharwal, P. Schniter, D. Guo, D. W. Bliss, S. Rangarajan and R. Wichman, "In-band full-duplex wireless: Challenges and opportunities," *IEEE J. Sel. Areas Commun.*, vol. 32, no. 9, pp. 1637-1652, Sept. 2014.
5. D. L. Pérez, X. Chu, A. V. Vasilakos and H. Claussen, "On distributed and coordinated resource allocation for interference mitigation in self-organizing LTE networks," *IEEE/ACM Trans. Netw.*, vol. 21, no. 4, pp. 1145-1158, Aug. 2013.
6. D. L. Pérez, X. Chu, A. V. Vasilakos and H. Claussen, "Power minimization based resource allocation for interference mitigation in OFDMA femtocell networks," *IEEE J. Sel. Areas Commun.*, vol. 32, no. 2, pp. 333-344, Aug. 2014.
7. M. Duarte, "Full-duplex wireless: Design, implementation and characterization," Ph.D. dissertation, Rice University, Houston, TX, USA, Apr. 2012.

8. T. Riihonen, S. Werner and R. Wichman, "Mitigation of loopback self-interference in full-duplex MIMO relays," *IEEE Trans. Signal Process.*, vol. 59, no. 12, pp. 5983-5993, Dec. 2011.
9. L. J. Rodríguez, N. H. Tran, and T. Le-Ngoc, "Optimal power allocation and capacity of full-duplex AF relaying under residual self-interference," *IEEE Wireless Commun. Lett.*, vol. 3, no. 2, pp. 233-236, Apr. 2014.
10. Z. Ding, I.Krikidis, B. Rong, J. Thompson, C. Wang and S. Yang, "On combating the half-duplex constraint in modern cooperative networks: Protocols and techniques," *IEEE Wireless Commun.*, vol. 19, no. 6, pp. 20-27, Dec. 2012.
11. S. Zhang, Q. F. Zhou, C. Kai and W. Zhang, "Full diversity physical-layer network coding in two-way relay channels with multiple antennas," *IEEE Trans. Wireless Commun.*, vol. 13, no. 8, pp. 4273-4282, Aug. 2014.
12. Y. Fan, C. Wang, J. Thompson and H. V. Poor, "Recovering multiplexing loss through successive relaying using repetition coding," *IEEE Trans. Wireless Commun.*, vol. 6, no. 12, pp. 4484-4493, Dec. 2007.
13. C. Wang, Y. Fan, J. Thompson and H. V. Poor, "A comprehensive study of repetition-coded protocols in multi-user multi-relay networks," *IEEE Trans. Wireless Commun.*, vol. 8, no. 8, pp. 4329-4339, Aug. 2009.
14. Y. Zhao, R. Adve and T. J. Lim, "Improving amplify-and-forward relay networks: optimal power allocation versus selection," *IEEE Trans. Wireless Commun.*, vol. 6, no. 8, pp. 3114-3123, Aug. 2007.
15. L. J. Rodríguez, N. H. Tran, A. Helmy and T. Le-Ngoc, "Optimal power adaptation for cooperative AF relaying with channel side information," *IEEE Trans. Veh. Technol.*, vol. 62, no. 7, pp. 3164-3174, Sept. 2013.
16. H. Kim, S. Lim, H. Wang and D. Hong, "Optimal power allocation and outage analysis for cognitive full duplex relay systems," *IEEE Trans. Wireless Commun.*, vol. 11, no. 10, pp. 3754-3795, Oct. 2012.
17. M. J. Emadi, A. G. Davoodi and M. R. Aref, "Analytical power allocation for a full-duplex decode-and-forward relay channel," *IET Commun.*, vol. 7, no. 13, pp. 1338-1347, Sept. 2013.
18. b. Yu, L. Yang, X. Cheng and R. Cao, "Power and location optimization for full-duplex decode-and-forward relaying," *IEEE Trans. Commun.*, vol. 63, no. 12, pp. 4743-4753, Dec. 2015.
19. G. Farhadi and N. C. Beaulieu, "Power-optimized amplify-and-forward multi-hop relaying systems," *IEEE Trans. Wireless Commun.*, vol. 8, no. 9, pp. 4634-4643, Sept.

- 2009.
20. M. Mohammadi, P. Sadeghi and M. Ardebilipour, "Node and symbol power allocation in time-varying amplify-and-forward dual-hop relay channels," *IEEE Trans. Veh. Technol.*, vol. 62, no. 1, pp. 432-439, Jan. 2013.
 21. Y. Hua, "An overview of beamforming and power allocation for MIMO relays," in *MILCOM*, San Jose, CA, USA, Nov. 2010, pp. 375-380.
 22. T. Riihonen, S. Werner and R. Wichman, "Hybrid full-duplex/half-duplex relaying with transmit power adaptation," *IEEE Trans. Wireless Commun.*, vol. 10, no. 9, pp. 3074-3085, Sept. 2011.
 23. L. Li, L. Wang and L. Hanzo, "Differential interference suppression aided three-stage concatenated successive relaying," *IEEE Trans. Commun.*, vol. 60, no. 8, pp. 2146-2155, Aug. 2012.
 24. H. Lu, P. Hong and K. Xue, "Generalized interrelay interference cancelation for two-path successive relaying systems," *IEEE Trans. Veh. Technol.*, vol. 63, no. 8, pp. 4113-4118, Oct. 2014.
 25. Y. Ji, C. Han, A. Wang and H. Shi, "Partial inter-relay interference cancellation in two path successive relay network," *IEEE Commun. Lett.*, vol. 18, no. 3, pp. 451-454, Mar. 2014.
 26. R. Zhang, "On achievable rates of two-path successive relaying," *IEEE Trans. Commun.*, vol. 57, no. 10, pp. 2914-2917, Oct. 2009.
 27. S. Gupta, R. Zhang and L. Hanzo, "Throughput maximization for a buffer-aided successive relaying network employing energy harvesting," *IEEE Trans. Veh. Technol.*, vol. 65, no. 8, pp. 6758-6765, Aug. 2016.
 28. C. Zhai, W. Zhang and P. C. Ching, "Cooperative spectrum sharing based on two-path successive relaying," *IEEE Trans. Commun.*, vol. 61, no. 6, pp. 2260-2270, Jun. 2013.
 29. L. Li, H. V. Poor and L. Hanzo "Non-coherent successive relaying and cooperation: principles, designs and applications," *IEEE Commun. Surveys Tuts.*, vol. 17, no. 3, pp. 1708-1737, 3rd quarter 2015.
 30. M. Lari, A. Mohammadi, A. Abdipour and I. Lee, "Characterization of effective capacity in AF relay systems," *IEICE Electron. Express*, vol. 9, no. 7, pp. 679-684, Apr. 2012.
 31. M. Lari, A. Mohammadi, A. Abdipour and I. Lee, "Characterization of effective capacity in antenna selection MIMO systems," *J. Commun. Netw.*, vol. 15, no. 5, pp. 476-485, Oct. 2013.
 32. M. Lari, "Effective capacity of receive antenna selection MIMO-OSTBC systems in co-channel interference," *J. Wireless Netw.*, DoI:10.1007/s11276-016-1219-x, Feb. 2016.

33. M. Lari, A. Mohammadi, A. Abdipour and I. Lee, "Effective capacity in receive antenna selection and spatially correlated MIMO-OSTBC systems," in *6th Int. Symp. Telecommun., (IST'12)*, Tehran, Iran, Nov. 2012, pp. 117-122.
34. N. Zhao, F. R. Yu, H. Sun and M. Li, "Adaptive power allocation schemes for spectrum sharing in interference-alignment-based cognitive radio networks," *IEEE Trans. Veh. Technol.*, vol. 65, no. 5, pp. 3700-3714, May. 2016.
35. X. Li, N. Zhao, Y. Sun and F. R. Yu, "Interference alignment based on antenna selection with imperfect channel state information in cognitive radio networks," *IEEE Trans. Veh. Technol.*, vol. 65, no. 7, pp. 5497-5511, Jul. 2016.
36. P. L. Yeoh, M. ElKashlan and I. B. Collings, "Selection relaying with transmit beamforming: A comparison of fixed and variable gain relaying," *IEEE Trans. Commun.*, vol. 59, no. 6, pp. 1720-1730, Jun. 2011.
37. I. S. Gradshteyn and I. M. Ryzhik, *Table of Integrals, Series, and Products*, 7th ed., Academic Press, 2007.
38. D. Wu and R. Negi, "Effective capacity: a wireless link model for support of quality of service," *IEEE Trans. Wireless Commun.*, vol. 2 no. 4, pp. 630-643, Jul. 2003.
39. B. Soret, C. A. Torres and J. T. Entrambasaguas, "Capacity with explicit delay guarantees for generic source over correlated Rayleigh channel," *IEEE Trans. Wireless Commun.*, vol. 9, no. 6, pp. 1901-1911, Jun. 2010.
40. X. Kang, Y. C. Liang and A. Nallanathan, "Optimal power allocation for fading channels in cognitive radio networks under transmit and interference power constraints," in *2008 IEEE Int. Conf. Commun., (ICC'08)*, Beijing, China, May. 2008, pp. 3568-3572.